CONF-890665--5

Performance of the Hermes-III Gamma Ray Simulator*

SAND--89-0031C

DE89 013068

Juan J. Ramirez, K. R. Prestwich, D. L. Johnson,
J. P. Corley, G. J. Denison, J. A. Alexander,
T. L. Franklin, P. J. Pankuch, T. W. L. Sanford,
T. J. Sheridan, L. L. Torrison, G. A. Zawadzkas
Sandia National Laboratories
Albuquerque, New Mexico 87185

Abstract

Hermes III is a 22-MV, 730-kA, 40-ns pulsed power accelerator that drives an electron beam diode/converter to generate an intense pulse of bremsstrahlung radiation. In Hermes III, eighty individual 1.1-MV, 220-kA pulses are generated and added in groups of four to develop twenty 1.1-MV, 730-kA pulses which are then fed through inductively isolated cavities and added in series by a magnetically insulated transmission line (MITL). An extension MITL delivers this summed output to the electron beam diode. The construction of Hermes III was completed February 1988 and was followed by an accelerator characterization and performance demonstration phase. Hermes III met all of its performance requirements during this testing period and has gone operational one year ahead of schedule. An overview of the Hermes-III design is presented together with details of the performance obtained for the various subsystems. A discussion of future applications of this technology is also presented.

Introduction

Hermes III is a 16-TW electron beam accelerator designed to generate an intense burst of bremsstrahlung radiation for the nuclear weapons effects simulation program at Sandia National Laboratories.[1] The design goal to deliver a minimum of 5 x 10^{12} Rads(Si)/sec over a cylindrical volume with a 500-cm^2 front surface area and 15-cm long has been exceeded. The radiation pulse has a 10/90 rise time and FWHM of ~20 ns. The dose rate is uniform within a factor of two along the front surface of the exposure volume and within a factor of four anywhere inside the test volume.

Hermes III represents a new class of accelerators that combine state-of-the-art pulsed power designs with high power linear induction accelerator cavities and voltage addition along an extended MITL. It is a major extension of the proof-of-principle HELIA experiment.[2] A drawing of Hermes III is shown in Fig. 1. At peak power, Hermes III delivers a 22-MV, 730-kA, 40-ns pulse to an electron beam

---

diode. It generates this output by adding the pulses produced by eighty pulse forming lines (PFLs) in a specific parallel/series combination. The eighty individual 1.1-MV, 220-kA PFL output pulses are first added in groups of four to generate twenty 1.1-MV, 730-kA pulses that are then fed through high power linear induction accelerator cavities. The induction cavities feed power along the length of a self-magnetically insulated vacuum transmission line, which adds the cavity outputs to generate the 22-MV, 730-kA, 40-ns pulse. The output of this adder MITL is delivered to the electron beam diode by an extension MITL. Figure 2 shows a cut-out view of the cavity/MITL system.

The eighty 1.1-MV pulses are generated by the synchronized switching of energy through several compression stages. The main energy store consists of ten 2.4-MV, 156-kJ Marx generators that are charged to ±95 kV DC. The energy from the Marx generators[3] is transferred, on command, to an intermediate energy store system consisting of twenty low inductance, water-dielectric capacitors. These self-contained coaxial units are arranged in pairs inside of two oil-filled tanks that also house the Marx generators. The water capacitors are charged to ~2.2 MV in ~950 ns.

The next compression stage is initiated by the command firing of twenty SF_6-insulated gas switches.[4] These switches are each triggered by a ~15-mJ laser pulse, and provide the overall synchronization of the accelerator. The output of a commercially available 900-mJ, 30-ns KrF laser is split into twenty beamlets that are appropriately delayed and directed to the individual gas switches. A drawing of the multi-stage gas switch is shown in Fig. 3. Each gas switch transfers energy from one water capacitor to four PFL modules. The PFLs are 5-ohm, coaxial, water dielectric transmission lines.[5] Each PFL module has a self-closing output switch, peaking switch, and crowbar switch. The output pulse amplitude and rise time are determined by the settings of the output and peaking gaps. The crowbar switch shorts the high voltage output electrode to ground and, thus, controls the output pulse width. A sketch of a PFL module is shown in Fig. 4.

Four PFL outputs are combined and fed to the MITL by one of the twenty induction cavities.[6] Figure 5 shows a cross section of the inductive cavities. Pairs of PFLs feed the left and right azimuthal transmission lines where their currents are summed. These summed pulses feed the inner azimuthal line where their currents are also added. The output of the inner azimuthal line is fed, thorough a vacuum insulator stack, to a vacuum transmission line that delivers the power to the adder MITL.

The outer conductor of the coaxial adder is formed by the surface of the cavity bores at a radius of 38.1 cm. This

surface is interrupted at regular intervals by the cavity feed gaps. The inner conductor of the adder is formed by a cantilevered cathode shank that is centered and aligned within the anode cylinder.[7] The cathode stalk decreases in radius at each cavity feed along the length of the MITL, thus increasing the impedance of each MITL section. A photograph of the cantilevered cathode stalk is shown in Fig. 6. The MITL system is a balanced design that requires equal power flow from each cavity.[8] This implies that the total current is constant through the system, and the impedance of the nth adder section is n-times the impedance of the first. The voltage at any location along the adder is thus given by the addition of the voltages fed by all the cavities up to that point. The extension MITL is a constant impedance coaxial system that provides a matched load to the adder. It includes a tapered section that reduces the dimensions of the MITL radii to match those of the electron beam diode.

The e-beam diode is shown in Fig. 7. It is a coaxial design with an annular cathode that terminates the long cantilevered cathode shank, and a flat plate anode that terminates the extension MITL. An optimized Ti/Ta/C target is used to convert the electron beam energy into bremsstrahlung radiation.[9]

Marx Generators And Intermediate Stores

Figure 8 shows a photograph of the installed Marx generators and intermediate energy store water capacitors. Each Marx generator is a duplicate of the first two rows of the PBFA-II Marx generator.[3] A 700-kV, 2.7-kJ Marx generator is used to trigger all five main Marx generators located in each of the two oil tanks. An oil transmission line network routes the output of the trigger Marx generator to the first row of the main Marx generators. The lengths of the oil transmission line segments are adjusted to erect the Marx generators in the proper sequence. The Marx generator system has proven very reliable. Four of the 1.3-μF, 100-kV capacitors have failed over the past two years of testing. Over 200,000 capacitor shots were accumulated over this period. The first-to-last spread observed on a typical shot for the ten Marx generators is ~35 ns.

The self-contained, 19-nF, coaxial water capacitors are arranged in pairs inside the two oil tanks. Each pair is furnished with a small volume water reservoir located above the top capacitor. This reservoir allows for volumetric changes resulting from deflections of the polyurethane barriers as the main oil tanks are filled and drained. The units are filled with deionized water and sealed off. The water resistivity decreases gradually over a period of time.

The rate at which the water resistivity decreases has slowed significantly over the past two years. At present, the capacitors are drained and refilled with deionized water once ever two weeks. The water resistivity decreases very little over this time period. The water capacitors have proven very reliable. No failures have been experienced to date.

Laser Triggered Gas Switches

The twenty laser-triggered gas switches provide the overall synchronization of Hermes III. The output of a commercially available 900-mJ, 30-ns FWHM KrF laser is split into twenty beamlets by the optical system and directed into the individual gas switches. The path lengths of the twenty beamlets are adjusted to provide the proper arrival time of the trigger pulse at the various switch locations.[10]

Figure 9 is a histogram of the first-to-last spread of the twenty gas switches as measured over a sequence of 400 shots. These data were taken at the nominal, 2.2 MV, operating voltage. The data can be represented by a Gaussian distribution with a mean spread of 8 ns. No attempt was made to optimize the switch performance during this shot sequence. Some of the systematic module-to-module timing differences can be removed from the data. Figure 10 shows the relative timing of the switches for six shots. The bottom three shots were taken after the laser path lengths were adjusted to compensate for those switches that appeared to be consistently early or late. When this was done, spreads of ~6 ns were obtained. This spread corresponds to an rms jitter for a single gas switch of 1.6 ns. Hermes III meets its output amplitude and pulse rise time requirements without the need to fine tune the spread of the gas switches beyond the level shown in Fig. 9. Under normal operating conditions, little effort is thus made to reduce the spread below the levels that are readily obtained. Details of the Hermes-III gas switch performance, together with initial measurements of the switch run time and jitter for various laser beam pulsewidths and energies, are presented by Denison, et al.[11]

Pulse Forming Lines

The Hermes-III PFL modules were developed in the Subsystems Test Facility (STF), and their performance capabilities have been reported earlier.[5] The module performance is dominated by reflections from impedance discontinuities at various places in the module. For optimum switch settings, the PFLs can produce a 1.3-MV, 260-kA, 40-ns pulse into a matched 5-ohm load with a 10/90 rise time of ~8 ns. On Hermes III, the eighty PFLs produce a mean peak output of 1.1 MV. Under these conditions, the typical

PFL output rise time is 12-15 ns. Some small module-to-module variability is seen in the wave shapes. Effort has not been made to remove systematic timing deviations by optimizing the switch settings. Hermes III meets or exceeds its overall output rise time specifications without the need to fine tune the performance of the PFLs.

The spreads of the time of arrival of the pulses at the output transmission lines (OTLs) were measured together with the gas switch closure spreads. The "effective" spread of the PFL switches is plotted in Fig. 11. These values were obtained by subtracting, in an approximate manner, the contribution from the gas switches. This was accomplished by calculating an rms jitter from the gas switch and OTL spreads, and assuming that

$$\sigma^2_{PFL} = \sigma^2_{OTL} - \sigma^2_{gas\ switch},$$

and then calculating the "effective" spread using these values for σ_{PFL}. The data is characterized by a Gaussian, with a mean spread of 18 ns and a sigma of 3.5 ns.[12] Tests performed over a short sequence of shots indicate that the width of this distribution can be narrowed significantly by carefully adjusting the switch settings. Measurements show that the radiation output, as given by the dose-area product, does not measureably decrease until the the PFL spread exceeds 30 ns.

The PFLs have provided reliable service after initial problems with poor weld joints were resolved. The most significant difficulty encountered with these units has been the occasional tracking of the oil/water barrier, located at the input of the PFL module. Some of the tracking appears to be related to the formation of bubbles on the barrier's surface, and some seem related to poor quality polyurethane material. Almost all of this tracking results in only a light amount of damage. Some barriers were left in place after the tracks were first observed and they continued to provide reliable operation for hundreds of subsequent shots. A minor modification to the barrier design appears to have resolved almost all of these problems.

Inductive Cavities

The performance of the inductive cavities is important in establishing the reliability of the overall accelerator. The maintenance of the vacuum insulator stack, that is located within each cavity, is important because these stacks cannot be cleaned or repaired in place and removal of a cavity is time-consuming. The insulators are lightly oiled before installation. We have inspected these insulators on several occasions over the past 16 months to monitor their condition.

Many of the insulators display a large number of very light surface tracks. Evidence of vacuum insulator flashover is not seen on any of the cavity waveforms during the main power pulse. Indications are that these light marks on the vacuum surface occur during the post-pulse ringing and do not carry much energy. It has only been necessary to remove a cavity to replace some insulator rings once to date with approximately 600 shots on those cavities. Two completely assembled cavities are kept as hot spares. It takes approximately three days to replace a cavity with one of the hot spares.

The High Voltage Adder

The performance of the high voltage MITL adder represented the highest technical risk in this accelerator design. The adder concept was demonstrated in the four-cavity HELIA experiment.[2] The major difference in the Hermes III design is that this system is long enough that a large section of the adder is transit time isolated from the load. The MITL thus works under self-limited conditions, whereas in the HELIA experiment, the system current was determined by the load.

The MITL is designed as a balanced system that requires equal power flow from each cavity. The same total current flows throughout the entire system, and the voltage at any point along the adder is the sum of the voltages of all the cavities up to that point. Figure 12 is a summary of the performance of the adder for a typical shot at ~19 MV. The total current is constant through the system. Three methods of estimating the voltages after the 4th, 8th, 12th, 16th, and 20th cavities are shown together with similar values for the diode.[13] As can be seen, the three estimates agree at all locations and demonstrate that the adder is working as designed.

The Diode And Radiation Output

The baseline Hermes-III diode uses an annular cathode and a planar anode. The operation of this diode has been described previously.[9] For anode-cathode (A-K) gaps greater than ~15 cm, the diode impedance is constant and is determined by the operating impedance of the MITL. The radius and angle of incidence of the annular beam at the anode surface is determined by the A-K gap. Figure 13 shows the time integrated dose produced by this diode, on the exterior surface of the converter (z=0), for an A-K gap of 37 cm. Because the beam is converging as it enters the converter, the radiation pulse is directed towards the axis. It peaks at ~z=5 cm to a maximum dose of ~160 kRads. This

corresponds to a peak dose rate of ~8 x 10^{12} Rads(Si)/sec. A number of variations of this diode are being investigated. One design which allows the beam to converge to a smaller radius in a short drift region between the anode and the converter has produced a peak dose rate of 1.7 x 10^{13} Rads(Si)/sec, with a FWHM pulse of ~13 ns, and a peak dose of 220 kRads over a 255 cm^2 area. Experiments are under way to optimize the performance of the various diode configurations.

Future Applications

Hermes III represents a 15-times scale up in power from HELIA (3 times the current and 5 times the voltage). We have developed design concepts that extend the Hermes-III technology in two directions.

EDNA is a concept for an Externally Driven Nuclear Assembly. It is projected to produce an intense burst of neutrons with a pulse width of 1-10 μs. The nuclear assembly is subprompt-critical, and multiplies the initial burst of neutrons produced by an accelerator. These neutrons can be produced by either the (γ,n) or (d,n) reactions on a suitable target. The pulsed power accelerator that is required for this application is a direct extrapolation of Hermes III. A comparison of relevant parameters is shown in Table I.

The Department of Energy is planning for a Laboratory Microfusion Facility (LMF) as the next major step in the national Inertial Confinement Fusion (ICF) program. Our concept of a light ion beam driver for the LMF is based on Hermes-III technology. Figure 14 is an artist's concept for the LMF. Each of the 32 LMF accelerator modules would deliver a ~32-MV, 1.2-MA, 54-ns pulse to a Li^+ extraction ion diode.[14] We project that 23 mJ of ion beam energy could be deposited in a 2-cm diameter target in 15 ns from this driver. A comparison of the LMF accelerator module and Hermes III is shown in Table II. The major difference is in the polarity of the adder MITL. For extraction ion diodes, the inner MITL conductor must operate in positive polarity. Results of positive polarity MITL experiments on Hermes III[15] and on HELIA[16] are presented at this Conference.

Summary And Conclusions

Hermes III is a very reliable electron beam accelerator, and generates the highest output voltage produced by a multi-terrawatt accelerator to date. It has met or exceeded all design specifications, and became operational one year ahead of schedule.

Work is under way to extend this technology to higher voltage electron beam accelerators for the Weapons Effects Simulation Program, and to high-power ion beam accelerators in the ICF program. One LMF accelerator module would deliver ~3 times the energy to an ion diode that Hermes III delivers to an electron beam diode, assuming that efficient coupling between the MITL and the ion diode is possible.

Acknowledgements

A large number of people contributed to the success of the Hermes III program. We wish to acknowledge especially the contributions of the assembly, test and operations team. Ian Smith proposed the initial HELIA concept. Pulsed Sciences Inc. designed the HELIA and Hermes III inductive cavities, and made key contributions to the development of the various bremsstrahlung sources being used in Hermes III.

References

1. J. J. Ramirez, et al., "Hermes III - A 16 TW, Short Pulse, Gamma Ray Simulator", in Proceedings of the 7th International Conf. on High Power Particle Beams, Karlsruhe, West Germany, July 4-8, 1988, pp. 148-157.

2. J. J. Ramirez, et al., "The Four Stage HELIA Experiment", in Proceedings of the 5th IEEE Pulsed Power Conf., Arlington, VA, June, 10-12, 1985, pp.143-146.

3. L. X. Schneider, "Development of a High Reliability 60 MV, 380 kJ Marx Generator," in Proceedings of the 4th IEEE Pulsed Power Conf., Albuquerque, NM, June 6-8, 1989, pp. 202-205.

4. G. J. Denison, et al., "A High Voltage Multistage Laser Triggered Gas Switch", in Proceedings of the 6th IEEE Pulsed Power Conf., Arlington, VA, June 29 - July 1, 1987, pp. 490-493.

5. J. P. Corley, et al., "Development and Testing of the Hermes III Pulse Forming Transmission Lines", ibid., pp. 486-489.

6. D. L. Johnson, et. al., "Hermes III Prototype Cavity Tests", ibid., pp. 482-485.

7. E. L. Burgess, et al., "Alignment of the Hermes III Magnetically Insulated Transmission Line.", ibid.. pp. 506-509.

8. R. C. Pate, et al., "Self-Magnetically Insulated Transmission Line System Design for the 20-Stage Hermes III Accelerator", ibid., pp. 478-481.

9. T. W. L. Sanford et al., "Tests of the Extended Planar Anode Diode on Hermes III", in Proceedings of the 7th International Conf. on High Power Particle Beams, Karlsruhe, West Germany, July 4-8, 1988, pp. 326-332.

10. R. A. Hamil, et al., "Laser Trigger System for the Hermes III Accelerator," in Proceedings of the 6th IEEE Pulsed Power Conf., Arlington, VA, June 29-July 1, 1987, pp. 526-528.

11. G. J. Denison, et. al., "Performance of the Hermes III Laser-Triggered Gas Switches", in these proceedings.

12. J. A. Alexander, et. al., "Performance of the Hermes III Pulse Forming Lines", in these proceedings.

13. T. W. L. Sanford, et. al., "Indirect Measurements of Hermes III Voltage", in Proceedings of the 1989 Particle Accelerator Conf., Chicago, IL, March 20-23, 1989.

14. D. L. Johnson, et al., "A Conceptual Design for an LMF Accelerator Module", ibid.

15. D. L. Johnson, et al., "Hermes III Positive Polarity Experiment", in these proceedings.

16. J. P. Corley, et al., "Positive Polarity Voltage Adder MITL Experiments on HELIA", in these proceedings.

*This work was supported by the U.S. Department of Energy under Contract De-AC04-76DP00789.

Figure Captions

Fig. 1 Drawing of the Hermes III accelerator.

Fig. 2 Cut-out view of Cavity/MITL system.

Fig. 3 Laser triggered, multistage gas switch.

Fig. 4 Drawing of the Hermes III PFL module.

Fig. 5 Inductive cavity cross section showing azimuthal transmission lines that add the currents from four PFL modules.

Fig. 6 Photograph of cantilevered cathode stalk.

Fig. 7 Schematic of annular electron beam diode with 18.5 cm diameter cylindrical cathode. The radiation pulse is produced when the electrons are stopped in the anode (target). Various radiation diagnostics, as well as typical electron trajectories, are shown.

Fig. 8 Photograph showing installed Marx generators and intermediate energy store capacitors.

Fig. 9 Histogram of first-to-last spread for the 20 gas switches over a 400 shot sequence.

Fig. 10 Relative gas switch timing for six shots. Bottom three shots have systematic timing differences removed.

Fig. 11 Calculate first-to-last spread of the 80 PFL switches over a 245 shot sequence.

Fig. 12 Schematic of high voltage adder together with measured currents and voltages at various locations along system.

Fig. 13 Time integrated dose produced by baseline diode with an A-K gap of 37 cm. The two curves represent the vertical and horizontal dose profiles.

Fig. 14 Design concept for a light ion beam LMF driver using 32 MV, 1.2 MA, 54 ns accelerator modules.

Table I.

Comparison of Hermes III and EDNA Accelerator Parameters.

EDNA	Hermes-III
40 cavities	20 cavities
160 PFLs, 4Ω, 60 ns	80 PFLs, 5Ω, 40 ns
1.2 MV cavity voltage	1.1 MV cavity voltage
47 MV output voltage	22 MV output voltage
1.2 MA total current	0.73 MA total current
3-5 shots per day	8-9 shots per day
37-m MITL	16-m MITL

Table II.

Comparison of Hermes III and LMF Accelerator Parameters.

LMF	Hermes III
32 cavities	20 cavities
128 PFLs, 4Ω, 54 ns	80 PFLs, 5Ω, 40 ns
Cavity Voltage (0.9 MV - 1.2 MV)	Cavity Voltage (1.1 MV)
Switch Jitter - 1σ	Switch Jitter - 1σ
gas --- 1.5 ns	gas --- 1.5 ns
water - 4.0 ns	water - 4.0 ns
Positive Adder MITL	Negative Adder MITL
Extraction ion diode	Extraction Electron Diode

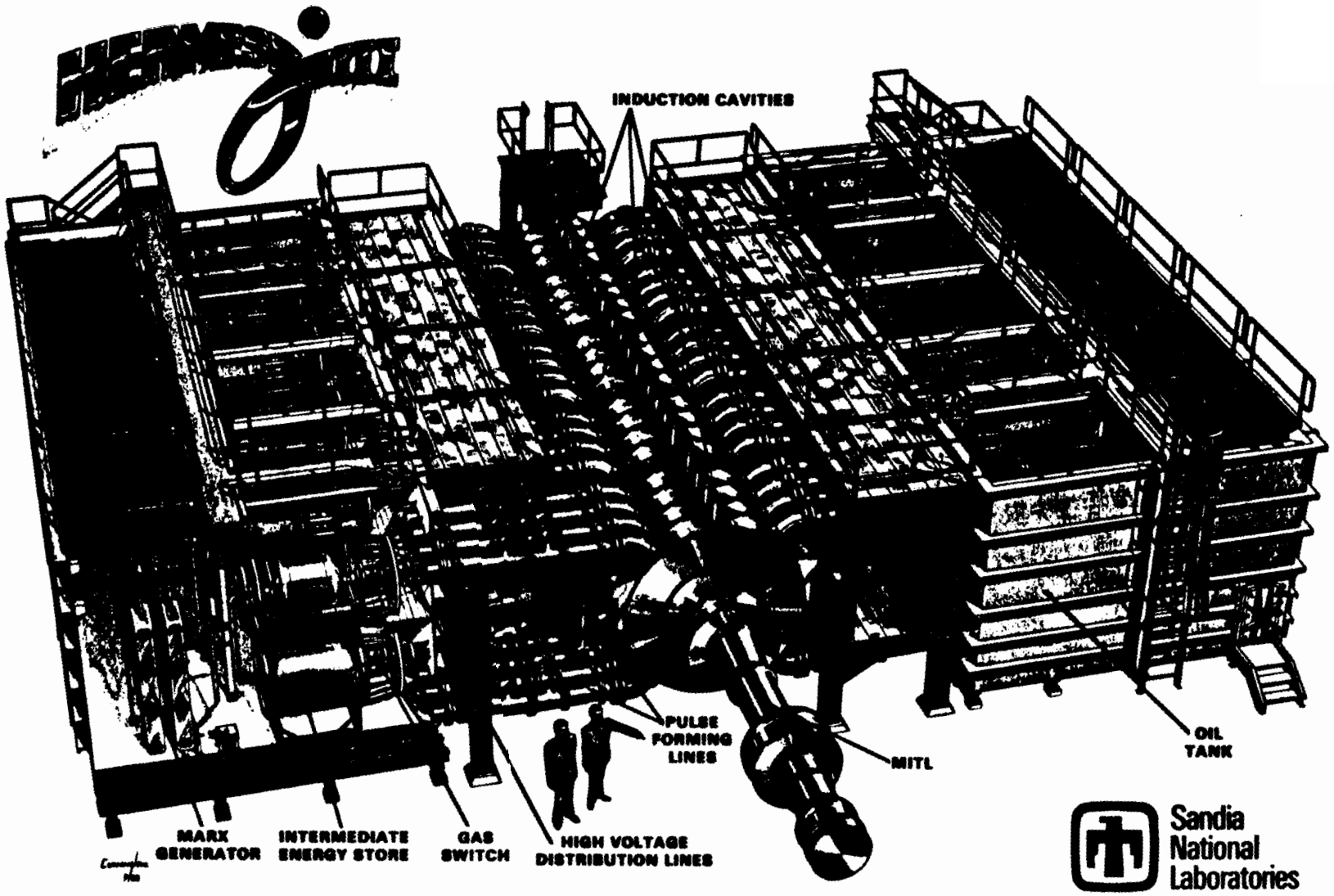

Figure 1

adder MITL

extension MITL

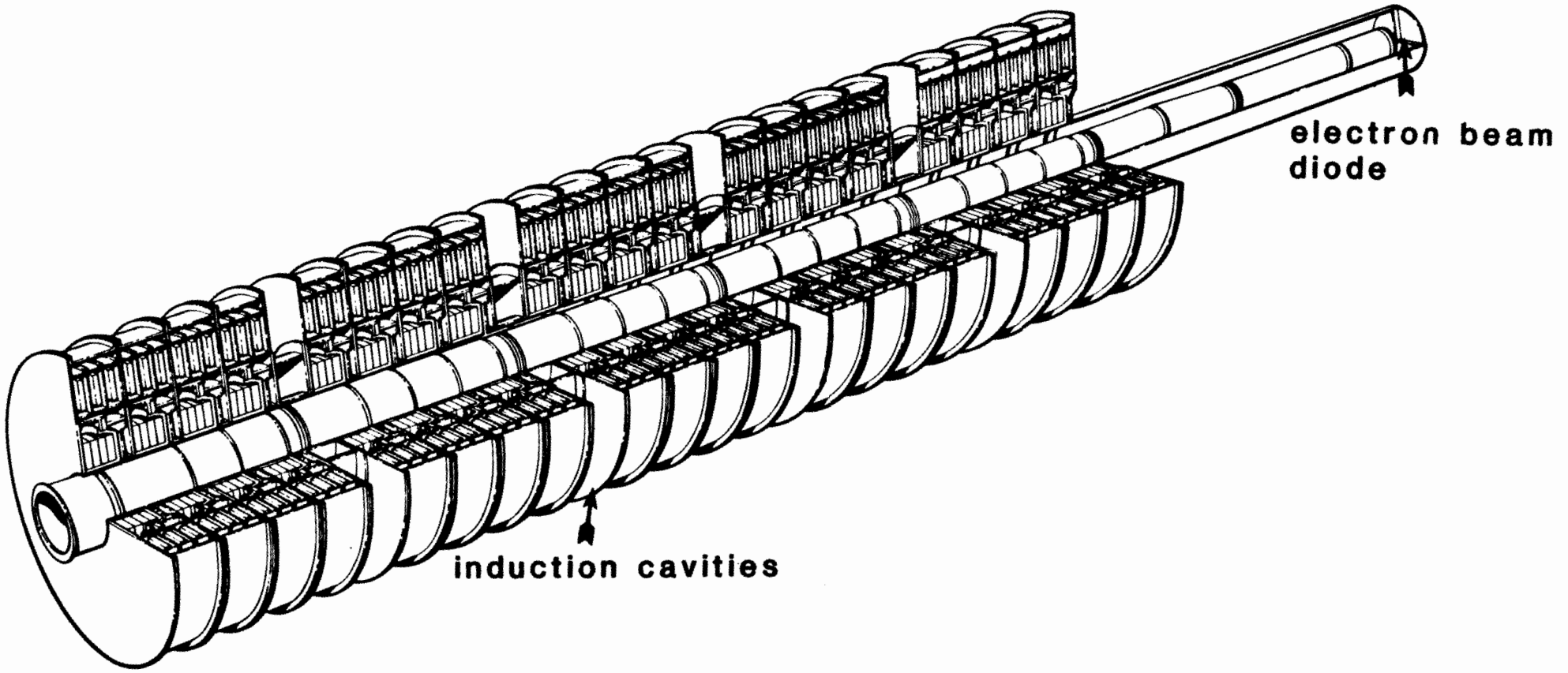

Figure 1

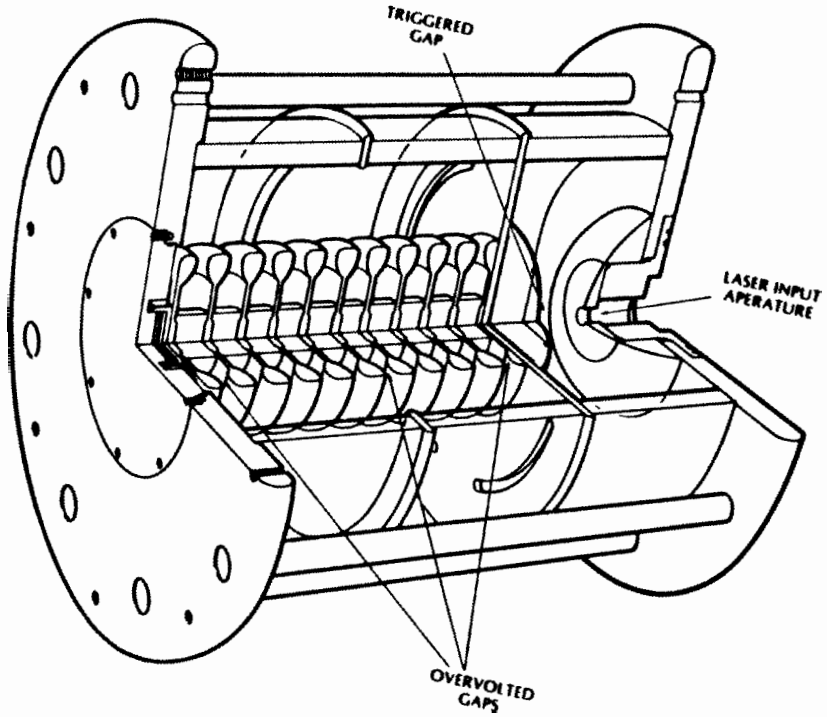

Figure 3

Fig 4 Drawing of PFL module

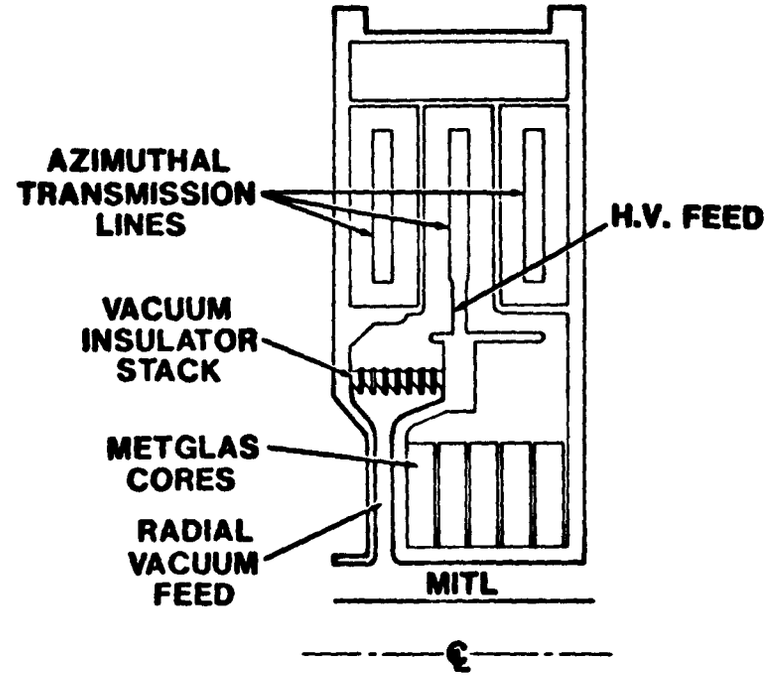
AZIMUTHAL
TRANSMISSION
LINES
H.V. FEED
VACUUM
INSULATOR
STACK
METGLAS
CORES
RADIAL
VACUUM
FEED
MITL
℄

Figure 5

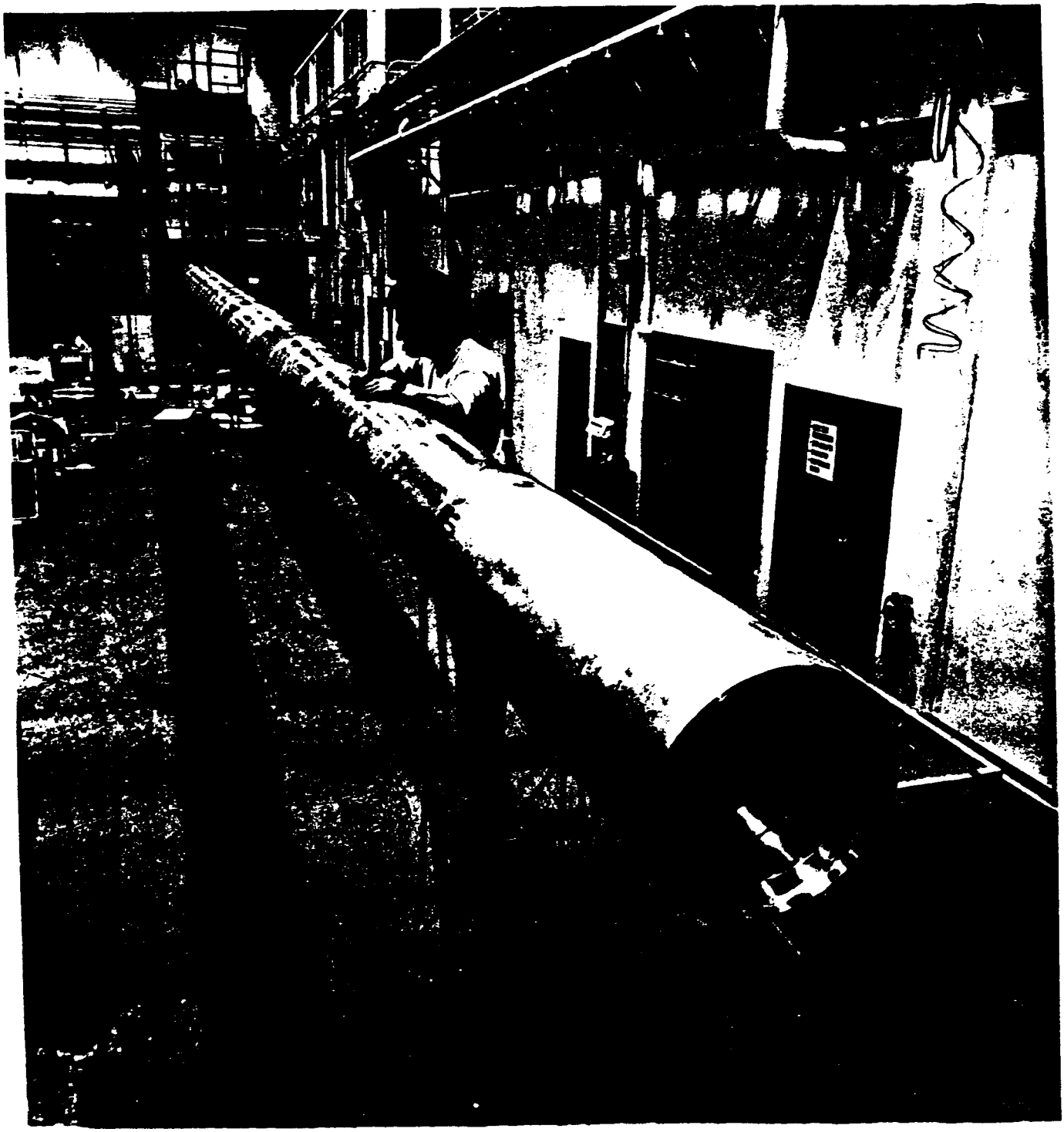

Figure 6

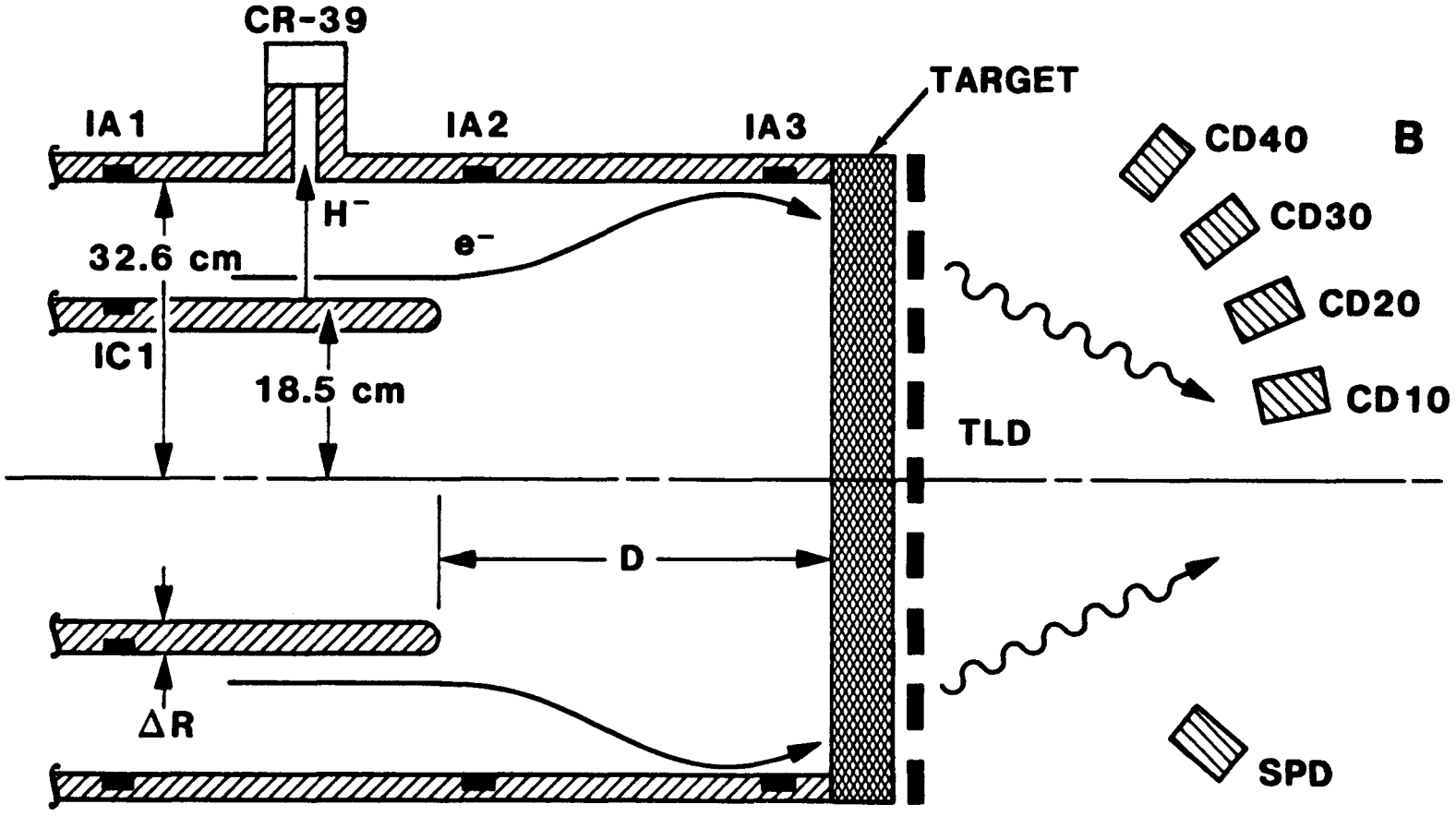
CR-39
TARGET
IA1
IA2
IA3
CD40
B
CD30
CD20
CD10
H⁻
e⁻
32.6 cm
IC1
18.5 cm
TLD
D
ΔR
SPD

Figure 1

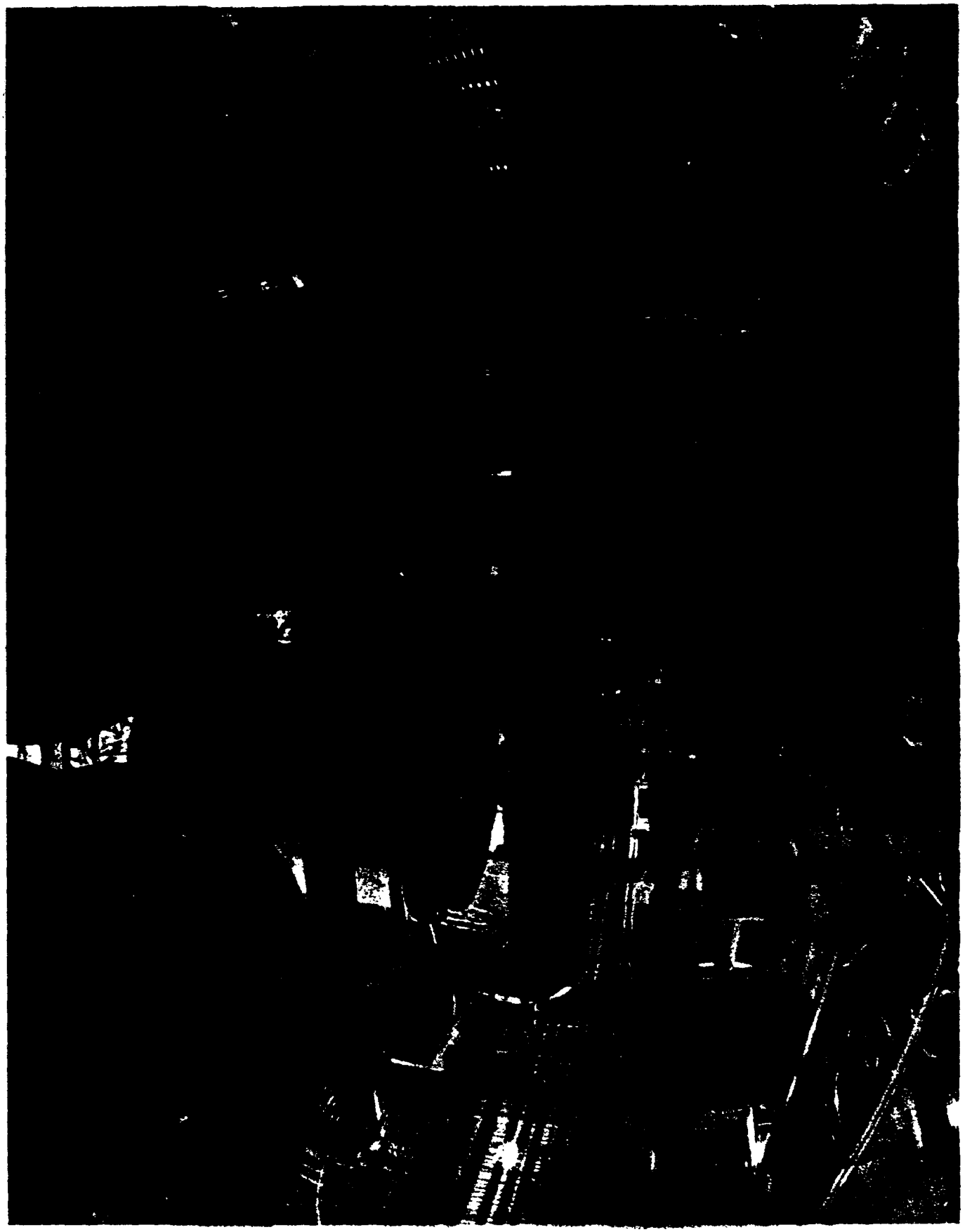

Figure 8

Fig 9

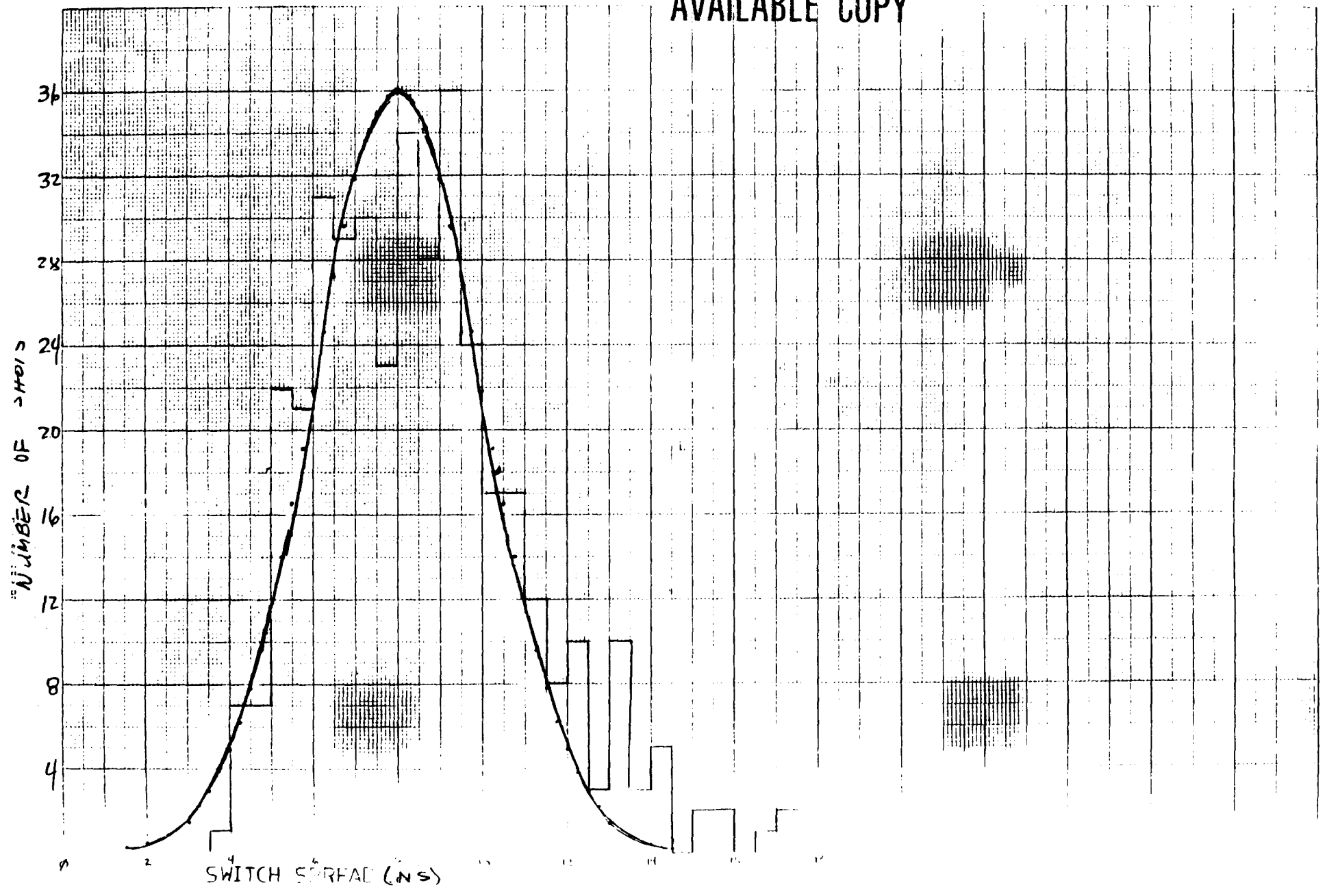

Fig 10. Relative gas switch T ~~—~~ for 6 shots
Bottom 3 shots have ~~[illegible]~~ systematic timing
differences removed

Fig 11

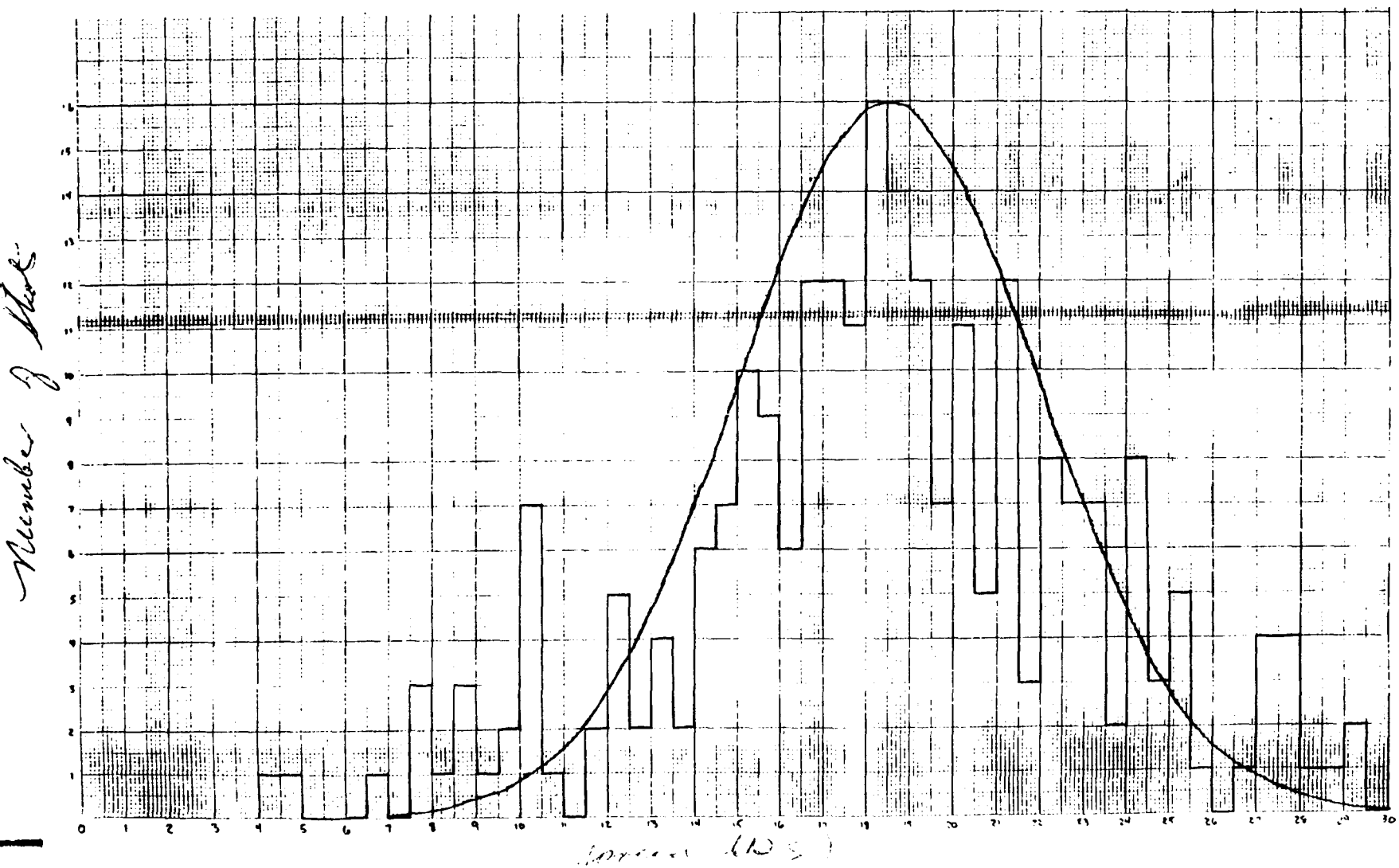

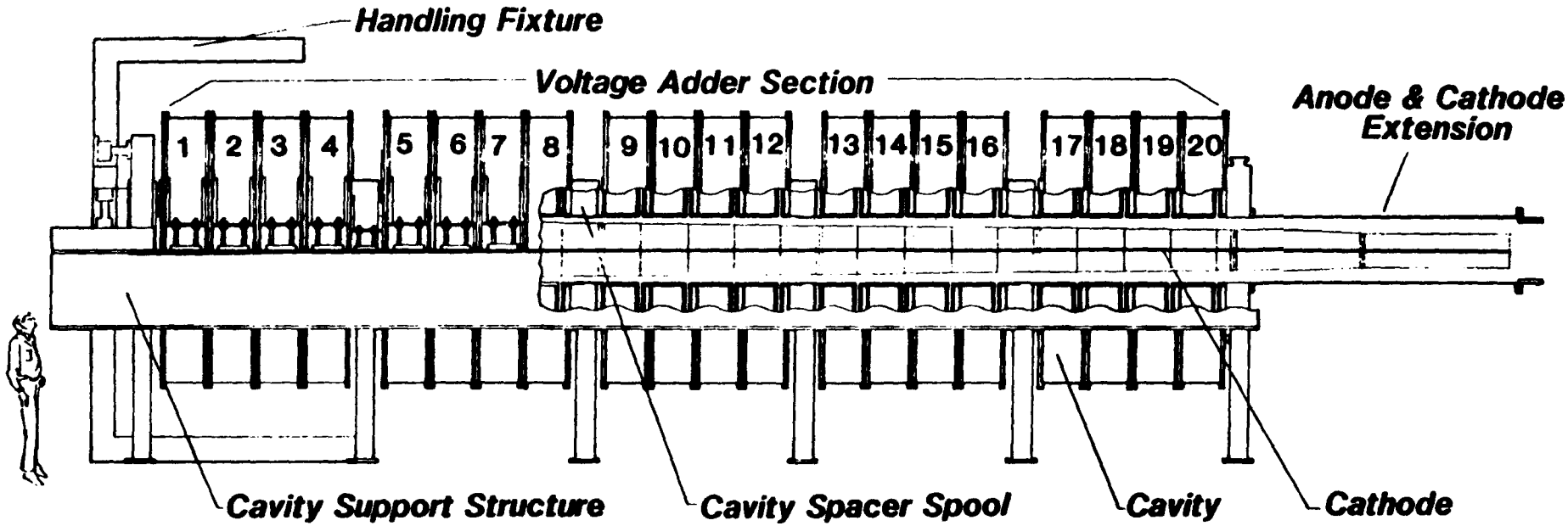

LOCATION	CAVITY 4	CAVITY 8	CAVITY 12	CAVITY 16	CAVITY 20	DIODE
I (kA)	683 ± 68	651 ± 65	662 ± 66	671 ± 67	681 ± 68	707 ± 71
V_{SCALED} (MV)	3.7	7.4	11.2	14.9	18.6	18.6
$V_{H-RANGE}$(MV)	3.6 ± .2	7.4 ± .2	11.0 ± .3	16.0 ± .4	18.5 ±.4	18.2 ± .4
$V_{PARAPOTENTIAL}$(MV)	3.7 ± .4	6.2 ± .6	11.7 ± 1.2	16.0 ± 1.6	17.9 ± 1.8	18.3 ± 1.8

$V_{CAVITY} = 0.93 \pm .04$ MV

Figure 12

HERMES III RADIATION DOSE PROFILE

Shot Number 545; Z= 0

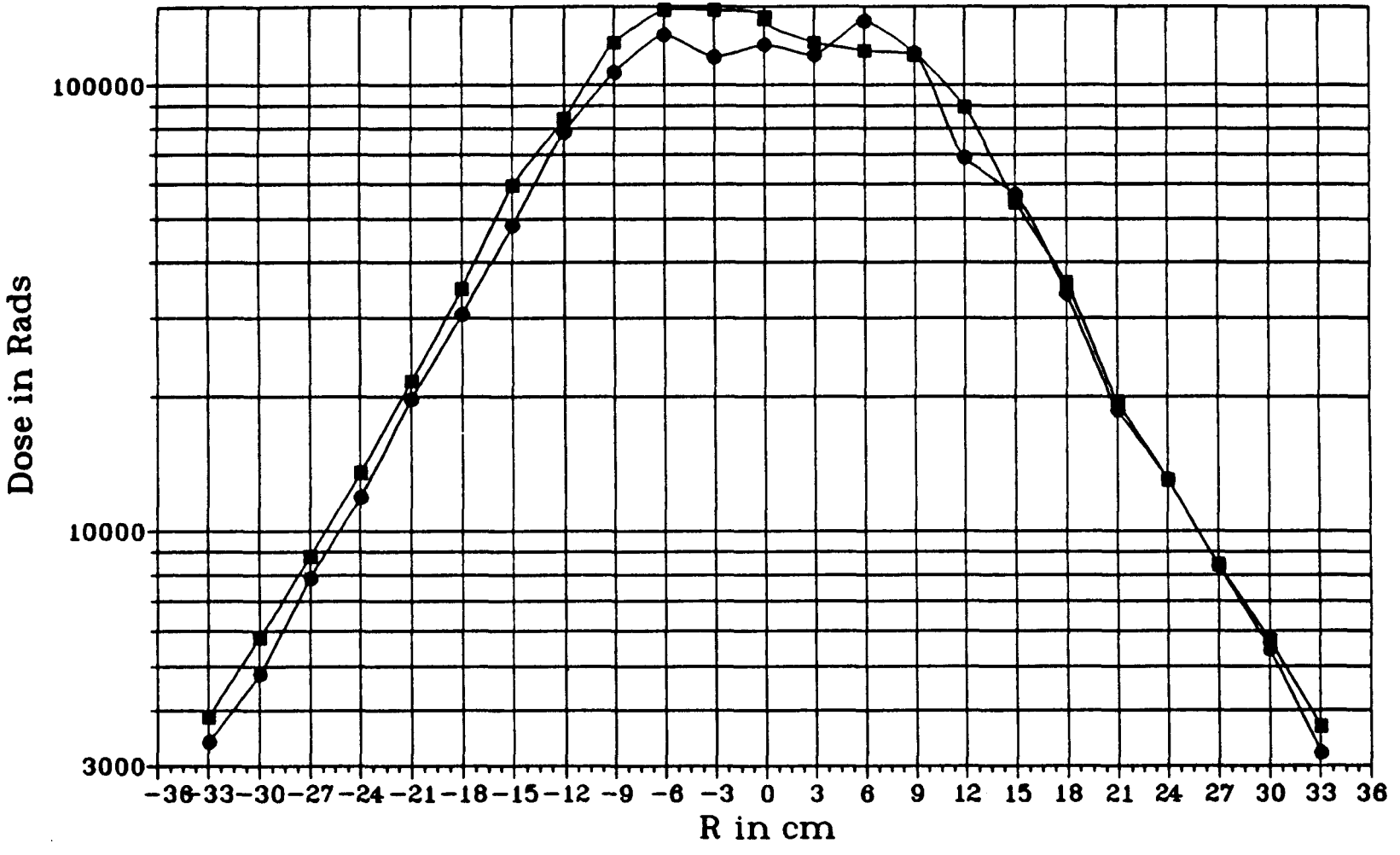

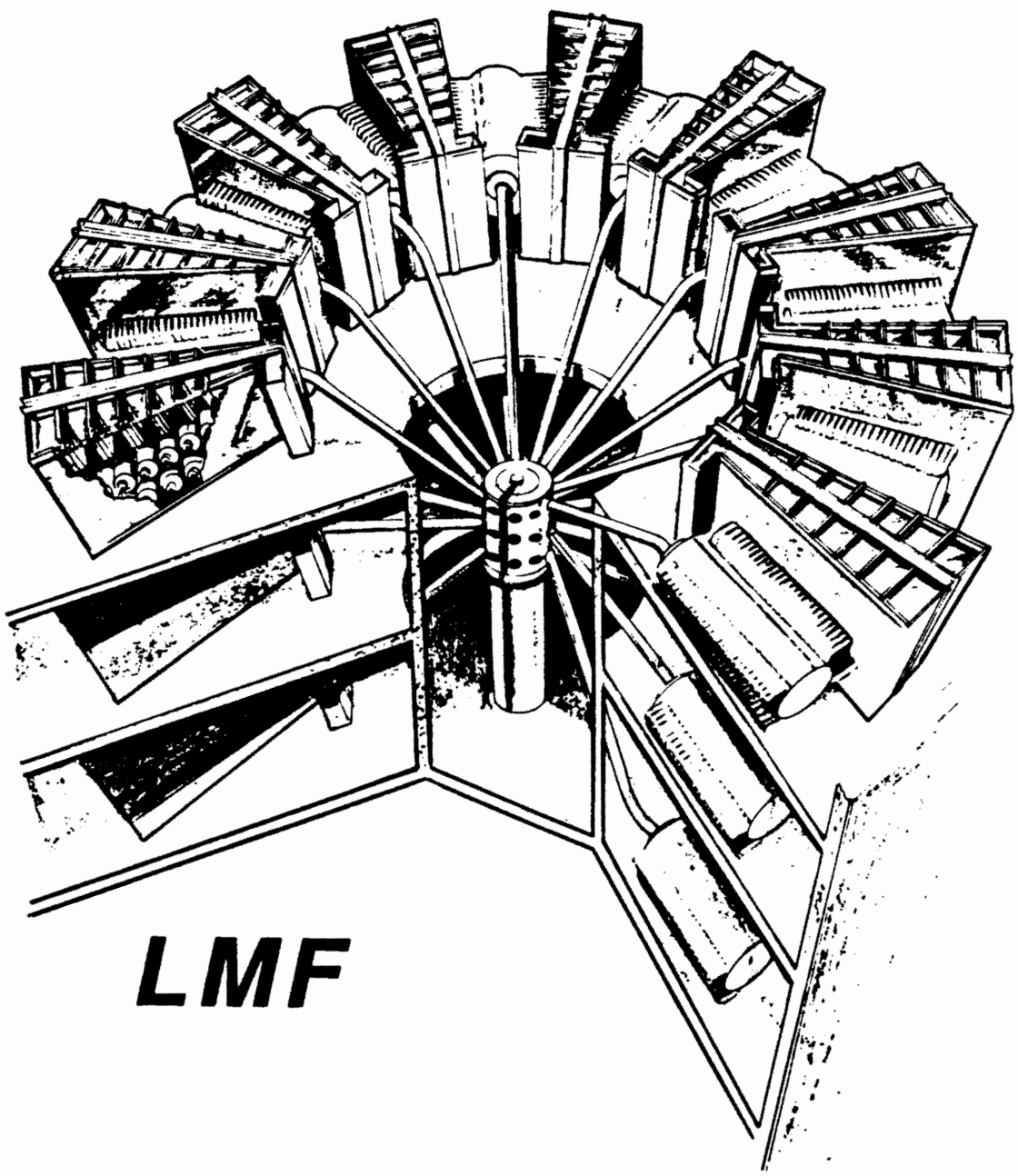

Figure 1c